Hindawi
Journal of Applied Mathematics
Volume 2020, Article ID 1073813, 7 pages
https://doi.org/10.1155/2020/1073813

Research Article

Harmonic Analysis via an Integral Equation: An Application to Dengue Transmission

R. G. U. I. Meththananda[1], **N. C. Ganegoda**[2], and **S. S. N. Perera**[3]

[1]*Department of Spatial Sciences, General Sir John Kotelawala Defence University, Southern Campus, Sooriyawewa, Sri Lanka*
[2]*Department of Mathematics, University of Sri Jayewardenepura, Nugegoda, Sri Lanka*
[3]*Department of Mathematics, University of Colombo, Colombo 03, Sri Lanka*

Correspondence should be addressed to N. C. Ganegoda; naleencg@gmail.com

Received 4 January 2020; Accepted 31 March 2020; Published 1 May 2020

Academic Editor: Fernando Simões

A collection of oscillatory basis functions generated via an integral equation is investigated here. This is a new approach in the harmonic analysis as we are able to interpret phenomena with damping and amplifying oscillations other than classical Fourier-like periodic waves. The proposed technique is tested with a data set of dengue incidence, where different types of influences prevail. An intermediate transform supported by the Laplace transform is available. It facilitates parameter estimation and strengthens the extraction of hidden influencing accumulations. This mechanistic work can be extended as a tool in signal processing that encounters oscillatory and accumulated effects.

1. Introduction

Harmonic analysis is central to many applications in signal processing. Its applicability does not restrict to physical waves, showing potential applications in many phenomena from biology to finance [1]. Superpositioning of basic waves to represent a wave or a function is the key mechanism in harmonic analysis. Fourier analysis is a frequently used method in signal processing, where sinusoidal waves perform as basis functions [2]. It is the baseline in many comparison studies as well. For instance, Broadbent and Maksik utilized the Walsh transform in analyzing rectangular waves [3].

In addition, statistical evaluations such as correlation analysis can also be adopted in studying signals, particularly time series. However, some details in multiple periodicities or unrecognized variables would not be extracted [4]. Thus, we opted to build our work advancing upon the Fourier series. Furthermore, there are techniques of accelerating convergence in the Fourier series, for instance, incorporating derivative information at the endpoints [5]. However, our approach allows changing harmonic patterns rather than restricting them into periodic waves.

As attributed to the Fourier series, periodic basis functions may not underlie every application. Therefore, variants with damping and amplifying oscillations would be subsequent improvements. Here, in this paper, we propose such work via the Volterra integral equation (1), which has been implemented to model population growth [6].

$$n(t) = n_0 f(t) + k\int_0^t f(t-\tau)n(\tau)d\tau. \tag{1}$$

The model equation (1) describes the population $n(t)$ according to the survival incorporated by a function $f(t)$ as age increases. It caters to an accumulated effect on the population as each surviving individual contributes to newborns. We alter its ideology into a context of epidemiology to mimic the incidence of infectious diseases. Then, an accumulated process of already infected individuals governs further incidence. Other external influences can also be incorporated.

We introduce a harmonic process carrying both sinusoidal and exponential effects to the solutions of (1). It endows with damping and amplifying oscillations other than to classical periodic waves. Next, we plan to extract influencing function $f(t)$ to understand the process behind each wave. This activity is further motivated by the difference kernel $kf(t-\tau)$ in (1), which leads to potential solutions for $n(t)$ via Laplace transforms. We validate this new harmonic analysis for dengue incidence with a comparison of the classical technique of discrete Fourier series.

2. Material and Methods

2.1. Preliminaries and Alterations to the Integral Model. In the exact terminology of the model equation (1), $n(t)$ is the total population at time t with an initial value n_0. Here, $f(t)$, the survival function, represents the fraction of people surviving to age t. Hence, $f(t)$ depicts the age-dependent potential of human survival, which is the main routine of the model. The parameter k represents the births per individual, and the argument $t-\tau$ in the kernel $kf(t-\tau)$ catches a lagging effect due to the time of birth.

In our move towards dengue incidence, $f(t)$ acts as an influencing function that tolerates ultimate transmission dynamics. For instance, when $n(t)$ detects the incidence, then $f(t)$ can represent an influencing factor such as rainfall patterns. Later, we aim to extract hidden influencing functions. Disease-specific interpretations can be aligned with the influences by vector mosquitoes, weather patterns, and biological or behavioral factors of human hosts [7].

Definition 1. We define $n(t)$ to be a measure on the number of infected cases (incidence) at time t influenced by an influencing function $f(t)$.

Our aim is to use $n(t)$ directly to formulate basis functions that approximate dengue incidence data.

Definition 2. We take $f(t)=\lambda e^{ct}\sin(at+b)$ to cater to damping $(c<0)$, amplifying $(c>0)$, or periodic $(c=0)$ oscillations in influencing functions.

The manipulation of $f(t)$ is twofold as articulating a sinusoidal pattern as a base and allowing damping and amplifying variants through exponential effects. Here, parameter a determines the wavelength or frequency and parameter b determines any shift due to initial requirements in the absence of an exponential effect. The role of the parameter λ is also twofold as standing for scaling requirements and partially responsible for the final linear combination of basic waves.

2.2. Model Solution. Now, we present the solution of the model equation (1) and its direction to the proposed application in dengue incidence.

Proposition 3. *The solution of (1) is given by* $n(t)=\mathscr{L}^{-1}\{(n_0\mathscr{L}\{f(t)\})/(1-k\mathscr{L}\{f(t)\})\}$, *and it has the following two cases for* $f(t)=\lambda e^{ct}\sin(at+b)$.

Case 1. (oscillatory solution). $n(t)=n_0\lambda e^{\beta t}(P\cos\mu t+Q\sin\mu t)$ where $\mu^2=a^2-k\lambda a\cos b-((k\lambda\sin b)/2)^2>0$, $P=\sin b$, $Q=(a\cos b+((k\lambda\sin^2 b)/2))/\mu$, and $\beta=c+((k\lambda\sin b)/2)$.

Case 2. (nonoscillatory solution): $n(t)=n_0\lambda e^{\beta t}(P\cosh\mu t+Q\sinh\mu t)$ where $-\mu^2=a^2-k\lambda a\cos b-((k\lambda\sin b)/2)^2>0$ and other formulas remain the same as in Case 1.

Proof. By applying the Laplace transform to (1) with the convolution property, we obtain $\mathscr{L}\{n(t)\}=n_0\mathscr{L}\{f(t)\}+k\mathscr{L}\{f(t)\}\mathscr{L}\{n(t)\}$, which provides $n(t)=\mathscr{L}^{-1}\{(n_0\mathscr{L}\{f(t)\})/(1-k\mathscr{L}\{f(t)\})\}$.

Since $\mathscr{L}\{f(t)\}=\lambda(((s-c)\sin b+a\cos b)/((s-c)^2+a^2))$, we arrive at

$$\mathscr{L}\{n(t)\}=n_0\lambda\frac{(s-c)\sin b+a\cos b}{\left((s-c-(k\lambda\sin b)/2)^2+a^2-k\lambda a\cos b-\left((k\lambda)^2\sin^2 b\right)/4\right)}. \quad (2)$$

If $a^2-k\lambda a\cos b-((k\lambda\sin b)/2)^2>0$, then we reach the solution in Case 1 and if $a^2-k\lambda a\cos b-((k\lambda\sin b)/2)^2<0$, then we have Case 2.

Next, Proposition 4 presents the inverse process of obtaining $f(t)$ that ensures the analytical existence of $f(t)$ for a given $n(t)$.

Proposition 4. $f(t)=\mathscr{L}^{-1}\{(\mathscr{L}\{n(t)\})/(n_0+k\mathscr{L}\{n(t)\})\}$.

Proof. The result is immediate by the earlier expression:

$$\mathscr{L}\{n(t)\}=n_0\mathscr{L}\{f(t)\}+k\mathscr{L}\{f(t)\}\mathscr{L}\{n(t)\}. \quad (3)$$

If the Laplace inverse is not straight forward, one would try Bromwich contour integrals [8, 9].

Definition 5. We structure the superposition upon $n(t)$ as $N(t)=\sum_{i=1}^{\infty}n_i(t)$, where $n_i(t)=n_{0i}\lambda_i e^{\beta_i t}(P_i\cos\mu_i t+Q_i\sin\mu_i t)$ is the basis function corresponding to the influencing function $f_i(t)=\lambda_i e^{c_i t}\sin(a_i t+b_i)$ for each case of $i=1,2,\cdots$. We call this $N(t)$ as an overall transmission potential.

Approximations in finite context can be obtained by $N_m(t)=\sum_{i=1}^{m}n_i(t)$, where m number of harmonics are used. This finally leads to approximate incidence data in the least square sense.

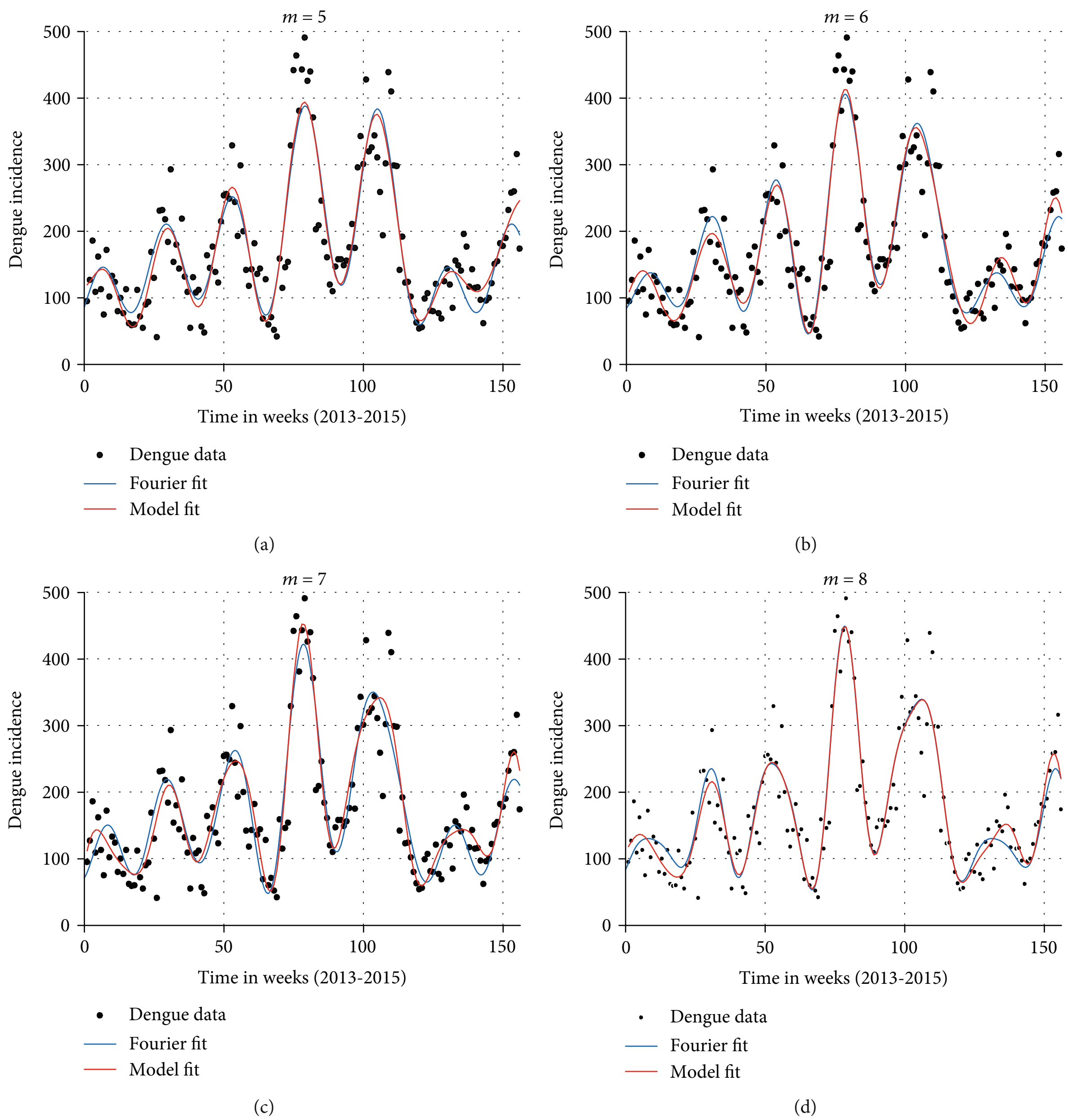

Figure 1: Dengue incidence data (dots), Fourier fit (blue curve), and model fit (red curve) for $m = 5, 6, 7, 8$.

2.3. Parameter Estimation. Since natural oscillations can be expected in epidemiological phenomena, we test with Case 1 of Proposition 3. Weekly dengue incidence data from 2013 to 2015 reported in the Colombo Municipal area, Sri Lanka [10] are used to extract basis functions and subsequently the influencing functions. This municipal area is highly vulnerable to dengue transmission due to the densely urbanized environment.

Suppose a trigonometric polynomial of order m, $T_m(t) = A_0 + \sum_{i=1}^{m} A_i \cos i\omega t + B_i \sin i\omega t$ is taken to approximate data in a discrete sense. First, we determine the Fourier harmonics $F_i(t) = A_i \cos i\omega t + B_i \sin i\omega t, i = 1, 2, \cdots, m$, and the intercept term A_0 (i.e., $F_0(t)$) using the MATLAB curve fitting toolbox that minimizes $\sum_{j=1}^{p} (d_j - T_m(t_j))^2$. Here, d_j refers to the data value at a point t_j for $j = 1, 2, \cdots, p$.

Next, we estimate initial guesses for each set of parameters of $f_i(t)$ infused in $n_i(t)$. These estimations are obtained by aligning $n_i(t)$ with sequential harmonics $F_i(t)$ separately. It is fulfilled by a trial and error method with a reasonable tolerance (ε) on the squared deviation between each $n_i(t)$ and its Fourier counterpart $F_i(t)$. Here, near-periodic behaviors are attributed into $n_i(t)$ while an exponential effect finally plays the role of fine-tuning the overall fit.

The following result guarantees that no complete restriction is employed on the exponential effect of $f_i(t)$ while forcing the removal of the exponential effect in the space of $n_i(t)$.

Proposition 6. *$\beta = 0$ does not necessarily imply $c = 0$.*

Table 1: Sum of squared deviation for $T_m(t)$ and $A_0 + N_m(t)$.

Number of harmonics (m)	Sum of squared deviations (in 10^5) $\sum_{j=1}^{p}(d_j - T_m(t_j))^2$	$\sum_{j=1}^{p}(d_j - (A_0 + N_m(t_j)))^2$
5	4.0969	3.6827
6	3.5767	3.2802
7	3.3986	2.9556
8	2.9763	2.7575

Proof. The result is straightforward as we have $\beta = c + ((\lambda k \sin b)/2)$.

Next, we initialize the parameters as described above and minimize $\sum_{j=1}^{p}(d_j - (A_0 + N_m(t_j)))^2$ that represents the deviation between data and superposition output $A_0 + N_m(t_j)$. For that, we implement a MATLAB fminsearch tool, which uses the Nelder-Mead simplex algorithm [11]. By using the resultant parameter values, we can determine all $n_i(t)$ and $f_i(t)$.

2.4. Outlook of Convergence. It is obvious that both the Fourier fit and the model fit yield better approximations of data when the number of series increases. For a given number of series, our model fit may reach data much closer than that of the Fourier fit by the effect of $e^{\beta_i t}$ in $n_i(t)$. It is assisted by the boundedness of t and the possibility of any real value for β_i. Note that the terms involving t in the Fourier fit are sine and cosine terms allowing only oscillations tolerated by respective coefficients. However, in the model fit, one may see the adaptability of coefficients as per the effect of $e^{\beta_i t}$. Options on β_i are indirectly subjected to the condition on μ_i^2 (Proposition 3). Notwithstanding, sophisticated searching abilities in the software may reduce its burden in computational trials.

3. Results

3.1. Curve Fitting. In Figure 1, Fourier fit $T_m(t)$ and model fit $A_0 + N_m(t)$ are illustrated. We add the intercept term A_0 into $N_m(t)$ to compromise with actual data. At the trial and error stage, the tolerance $\varepsilon < 10^3$. We start with $m = 5$ and finish with $m = 8$, which is the maximum number of harmonics allowed in the MATLAB Fourier fit.

Graphs in Figure 1 visualize the reliability of the fitted curves for different m, and Table 1 contains the sum of squared deviations. It shows that $A_0 + N_m(t)$ fits well compared to its corresponding $T_m(t)$ for each m. Therefore, the basis function $n_i(t)$ can further be used as a reliable intermediate tool to extract $f_i(t)$.

One can observe that the model fit and the Fourier fit mainly differ at the extremes of the data set. It is an optimistic rectification over Fourier harmonics to achieve a better fit via the model (1). This hints the effect of $e^{\beta_i t}$ in $n_i(t)$ as discussed in Section 2.4. Figure 2 further illustrates such an effect at an extreme. Here, the red curve stands for $\cos t + 0.5 \sin t$ and the blue curve $e^{0.1t}(\cos t + 0.5 \sin t)$ contains an exponential effect. Observe that the additional fluctuations of the blue

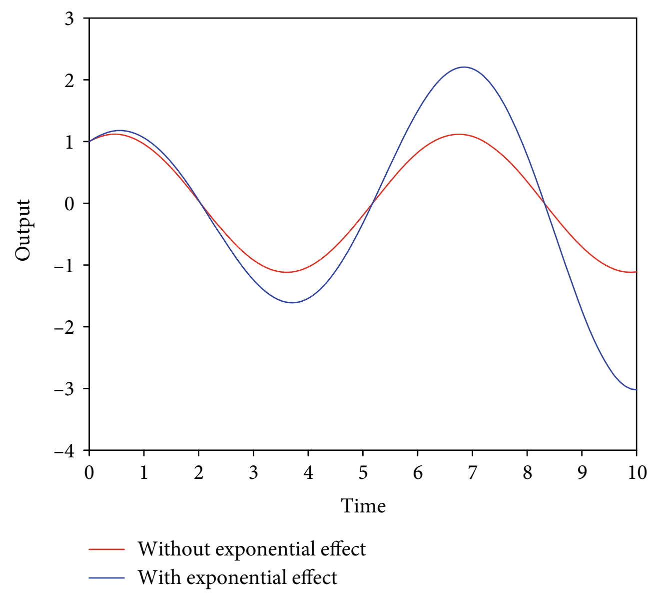

Figure 2: Comparison of the harmonic curve with and without an exponential effect.

curve at the latter stage allow for reaching attributes in data, which cannot be extracted only via sinusoidal curves. Thus, the convergence of series at extremes is more equipped with exponential orders.

3.2. Basis Functions. Since improvements are expected upon near-periodic waves, it is worthwhile to see the deviations in trigonometric terms. Figure 3 depicts the relevant cases in each harmonic for $m = 5$. We illustrate sine terms (a_1-a_5) and cosine terms (b_1-b_5) in the Fourier fit and their counterparts in the model fit, excluding the exponential effect. Besides, harmonics are also presented without A_0 (Figure 3, c_1-c_5). The values of $i\omega$ and μ are indicated to see the variations.

Here, different oscillatory behaviors are visible as damping where $\beta < 0$ (c_1, c_3, c_4, and c_5) and amplifying where $\beta > 0$ (c_2). The strength of the damping or amplifying nature can be seen via the size of β. Thus, comparatively large $|\beta|$ forces the curves to deviate from the classical periodic nature. Oscillations around zero preserve the same argument as in Fourier harmonics, which indicate changes over an intercept value A_0.

In the final model fit, parameter λ is partially responsible for combining basic patterns of the type $e^{\beta t}(P \cos \mu t + Q \sin \mu t)$. Originally, λ determines the amplitude (scaling) requirements of influencing pattern $e^{ct} \sin(at + b)$. Besides, parameter n_0 stands for further compromise of the amplitude while representing the initial requirements of the model (1). These parameter values for the above case in Figure 3 are listed in Table 2. The values of $n_0\lambda$ are also displayed to see the outcome of combining $e^{\beta t}(P \cos \mu t + Q \sin \mu t)$ type waves in the overall transmission potential. Thus, our approach establishes a mechanistic way of seeing different possibilities of oscillatory harmonics.

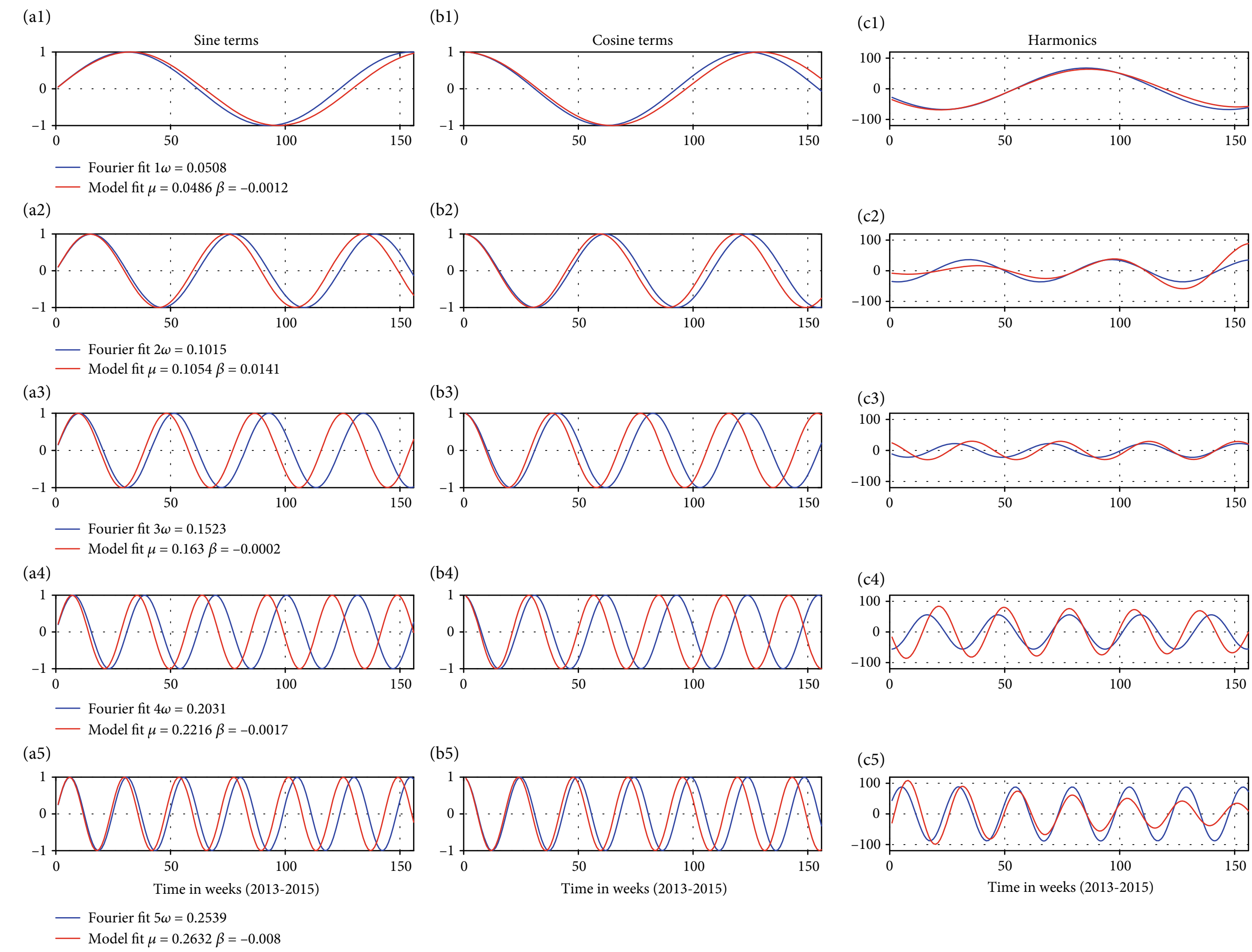

Figure 3: Behavior of sine terms, cosine terms, the Fourier fit (without A_0), and the model fit (without A_0) for $m = 5$. (a_i), (b_i), and (c_i) correspond to the i^{th} harmonic n_i, $i = 1, 2, \cdots, 5$.

Table 2: Parameters λ and n_0 of harmonics.

Harmonic	λ	n_0	$n_0\lambda$
n_1	-0.7135	95.5996	-68.2103
n_2	0.6764	14.3786	9.7257
n_3	-4.3978	6.8828	-30.2692
n_4	0.9159	114.5023	104.8727
n_5	1.1184	106.8252	119.4733

Table 3: Coefficients $n_0\lambda P$ and $n_0\lambda Q$.

Harmonic	$n_0\lambda P$	$n_0\lambda Q$	$\lvert n_0\lambda P\rvert + \lvert n_0\lambda Q\rvert$
n_1	-32.5710	-62.5813	95.1523
n_2	-7.3502	-6.5090	13.8593
n_3	26.7907	-13.3628	40.1536
n_4	2.3282	-87.1692	89.4974
n_5	-57.8863	100.9381	158.8243

According to the size of $n_0\lambda$, n_2 and n_5 contain the lowest impact and the highest impact, respectively, for the overall transmission. Such observations allow for seeing the quality (via the positive/negative sign of $n_0\lambda$) and the quantity (via the size of $n_0\lambda$) of contributions made by each harmonic structure $e^{\beta t}(P\cos\mu t + Q\sin\mu t)$.

Analogous to Fourier analysis, one can design a power spectrum by summing the size of coefficients in each exponentially weighted sinusoidal: $e^{\beta t}\cos\mu t$ and $e^{\beta t}\sin\mu t$. Table 3 contains those coefficient values and the power taken as $|n_0\lambda P| + |n_0\lambda Q|$. Here, also n_2 and n_5 contain the lowest power and the highest power, respectively.

Decomposing a data series into basic sinusoidal waves is the main routine of Fourier analysis. Similarly, our approach via model (1) accompanies a structure with exponentially weighted sinusoidals. A noted fact is that in influencing functions also, we can observe a similar context of exponentially weighted sinusoidal.

3.3. Influencing Functions. The influencing functions $f_i(t)$ of the above case in Figure 3 are shown in Figure 4. As described earlier, these functions incorporate accumulation effects of influences on disease transmission. Note that if no accumulation is enforced (i.e., $k = 0$), then the behavior of the basis

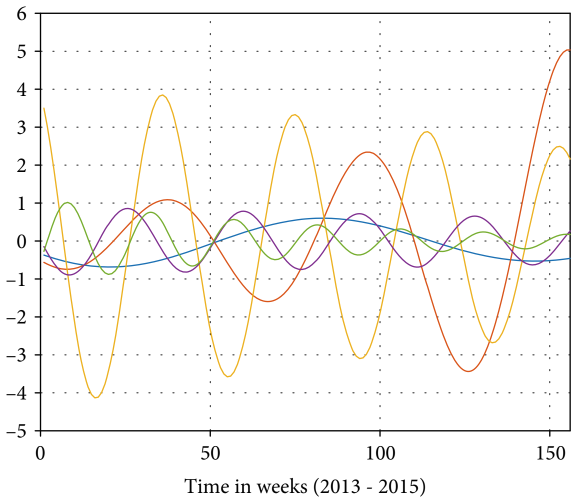

Figure 4: Influencing functions for $m = 5$.

function is a direct implication of corresponding influencing function since $n(t) = n_0 f(t)$ by (1). The strength of the accumulation can also be estimated via the size of k. According to the displayed values of k, f_3 and f_4 contain the lowest impact and the highest impact on the accumulations, respectively.

Different oscillatory behaviors can be seen as damping, where $c < 0$ (f_1, f_3, f_4, f_5), and amplifying, where $c > 0$ (f_2). Here, also, we observe the quality (via the positive/negative sign of k) and the quantity (via the size of k) of contributions made by the accumulation $\int_0^t f(t-\tau)n(\tau)d\tau$ in model equation (1).

3.4. Interpretation Prospects. Dengue is a mosquito-borne viral disease, which is caused by four virus serotypes (DENV-1, DENV-2, DENV-3, and DENV-4). Long-term exposure to one serotype generates immunity to that particular type, but only partial cross-protection is evident for other serotypes in the long run [12, 13]. On the other hand, vector mosquitoes, *Aedes aegypti* and *Aedes albopictus*, are highly adapted to the urban environment [14, 15]. Therefore, a collective risk may occur in different combinations of virus types and adapted mosquitoes. This leaves control measures unstable and inconsistent, which can be identified by amplifying oscillations in basis functions (e.g., n_2).

After a set of individuals are infected with dengue, their transmission capability fluctuates in different ways. As damping oscillations suggest, that capability may feature in two ways as aligning with rainfall patterns and aligning with awareness on disease control. Since awareness increases in rainy seasons, that combined effect is subject to oscillatory behavior. The concerned Colombo municipal area is vulnerable to a peak in rainfall in every six months due to monsoon and intermonsoon effects [16]. Therefore, as seen in (c_4) and (c_5), we may expect a peak in transmission around every six months. Meanwhile, as shown in (c_1), n_1 captures a higher incidence in the middle period of the data series, suggesting the capability of incorporating long-term influences.

The basis function n_3 in (c_3) does not indicate strong peaks but suggests a quicker saturation to a particular transmission level. This is understood via improved mosquito control and health care irrespective of rainfall effects. More specific interpretations can be drawn when we consider more harmonics in T_m and correspondingly in N_m. On the other hand, one can keep the desired information while removing any noisy or extraneous waves when we have more harmonics [1].

4. Discussion and Conclusion

A mechanism for extracting oscillatory behaviors with damping, amplifying, or periodic nature is discussed in this work. It is contrasting to the classical harmonic analysis by Fourier series, where only periodic waves are considered. The integral equation (1) allows the dependent variable to incorporate accumulation over a time period. Incidence of infectious diseases such as dengue can be modeled similarly as in (1). The whole work amalgamates decomposing data into basic oscillatory waves and infusing accumulation into those waves.

The difference kernel in (1) leads to the easier implementation of convolution property in the Laplace transform. We consider oscillatory basis functions according to the choice of influencing functions (Proposition 3). Our approach for parameter estimation aligns with near-periodic harmonics. Proposition 6 supports the existence of all oscillatory types for influencing functions though we impose near-periodic patterns for corresponding basis functions. In a theoretical sense, Proposition 4 guarantees a transform between basis functions and influencing functions. The Laplace transform entitles with numerous classes of problems, including differential equations, frequency analysis, and circuit analysis [17]. Our work also shows the importance of its intermediate role in bridging a model solution to harmonic analysis.

Overall, transmission potential $N(t)$ assimilates dengue incidence better than its Fourier counterpart, as shown in Table 1. Subject to trialing with Fourier waves for initial guesses, we tend to fine-tune the overall behavior via an exponential effect in each basis function. Different combinations of influences for dengue transmissions can be interpreted via resultant harmonics. In particular, damping oscillations may extract the combined influence of rainfall and awareness on disease control. The amplifying oscillations would show the variations in transmission due to different virus types and adapted mosquitoes. Extraction of responsible influencing functions, along with their contribution to accumulation, leads to more disease-specific interpretations. Cumulative effects are not restricted to one disease or one phenomenon. As White et al. [18] presented, for a general health impact, one must go beyond disease-specific models. Thus, a work similar to here can be extended to investigate accumulation cum harmonic effects.

The model-based harmonic analysis proposed here can be extended for applications outside epidemiology too. Any phenomena having meaningful oscillatory basic waves influenced by accumulation effects are the potential candidates for that.

Data Availability

Data can be retrieved via Epidemiology Unit, Ministry of Health, Sri Lanka, Available at: http://www.epid.gov.lk.

Conflicts of Interest

The authors declare that they have no conflicts of interest.

References

[1] J. Candy, *Signal processing*, John Wiley & Sons Inc, USA, 2006.

[2] W. Press, S. Teukolsky, W. Vetterling, and B. Flannery, *Numerical Recipes in C*, Cambridge University Press, Cambridge, 1992.

[3] H. A. Broadbent and Y. A. Maksik, "Analysis of periodic data using Walsh functions," *Behavior Research Methods, Instruments, & Computers*, vol. 24, no. 2, pp. 238–247, 1992.

[4] M. Filipowich, *What are the advantages & disadvantages of correlation research?*March 2020, https://classroom.synonym.com/advantages-disadvantages-correlation-research-8359597.html.

[5] W. Li, "Alternative Fourier Series Expansions with Accelerated Convergence," *Applied Mathematics*, vol. 7, no. 15, pp. 1824–1845, 2016.

[6] A. Jerri, *Introduction to Integral Equations with Applications*, Dekker, New York, 1985.

[7] N. C. Grassly and C. Fraser, "Mathematical models of infectious disease transmission," *Nature Reviews Microbiology*, vol. 6, no. 6, pp. 477–487, 2008.

[8] G. Milovanovic and A. Cvetkovic, "Numerical inversion of the Laplace transform," *Facta universitatis - series: Electronics and Energetics*, vol. 18, no. 3, pp. 515–530, 2005.

[9] P. W. Fernando and S. S. Sritharan, "Non-detection probability of diffusing targets in the presence of a moving searcher," *Communications on Stochastic Analysis*, vol. 8, no. 2, 2014.

[10] Epidemiology Unit, *Ministry of Health, Sri Lanka*October 2019, http://www.epid.gov.lk.

[11] J. C. Lagarias, J. A. Reeds, M. H. Wright, and P. E. Wright, "Convergence properties of the Nelder–Mead simplex method in low dimensions," *SIAM Journal on Optimization*, vol. 9, no. 1, pp. 112–147, 1998.

[12] L. Esteva and C. Vargas, "Coexistence of different serotypes of dengue virus," *Journal of Mathematical Biology*, vol. 46, no. 1, pp. 31–47, 2003.

[13] N. G. Reich, S. Shrestha, A. A. King et al., "Interactions between serotypes of dengue highlight epidemiological impact of cross-immunity," *Journal of The Royal Society Interface*, vol. 10, no. 86, article 20130414, 2013.

[14] World Health Organization, *Dengue fever - Sri Lanka*November 2019, https://www.who.int/csr/don/19-july-2017-dengue-sri-lanka/en/.

[15] P. Sirisena and F. Noordeen, "Evolution of dengue in Sri Lanka—changes in the virus, vector, and climate," *International Journal of Infectious Diseases*, vol. 19, pp. 6–12, 2014.

[16] D. W. T. T. Darshika, I. M. S. P. Jayawardana, and D. M. S. C. Dissanayake, "Multi model ensemble climate change projections for annual and seasonal rainfall in Sri Lanka," *Sri Lanka Journal of Meteorology*, vol. 3, pp. 19–27, 2018.

[17] ScienceDirect, *Laplace transform*March 2020, https://www.sciencedirect.com/topics/engineering/laplace-transforms.

[18] H. White, P. O'Campo, R. Moineddin, and F. Matheson, "Modeling the cumulative effects of social exposures on health: moving beyond disease-specific models," *International Journal of Environmental Research and Public Health*, vol. 10, no. 4, pp. 1186–1201, 2013.